

Figure 1. (A) Traditional condensation ammonia synthesis process compared to (B) the absorbent-enhanced ammonia-synthesis process.

absorption using supported metal halides as shown in Figure 1.<sup>2,8,11–14</sup> Here, “absorption” refers to the process of incorporating the target species, ammonia, into the lattice structure of the absorbent material; alternatively, “adsorption” refers to the binding of a target molecule onto the surface of a solid sorbent. Absorption in salts is more selective than adsorption and offers a larger volumetric separation capacity than adsorption in zeolites or MOFs, even at higher temperatures approaching those of ammonia synthesis reaction.<sup>15,16</sup> An advantage of the absorbent-enhanced Haber–Bosch process (Figure 1B) is that it can remove ammonia more completely than condensation while still achieving production rates similar to that of the condenser process at lower pressure.<sup>10</sup> As a result, it requires less compression work, lower capital costs, and less energy for operation. In this way, the use of supported metal halides (e.g.,  $MgCl_2$ ) to capture ammonia in an ammonia synthesis process offers potential for a more sustainable and economical renewable ammonia synthesis at a small production scale.<sup>6,10,17,18</sup>

While capturing ammonia using metal halides can be more economical and efficient compared to the condensation approach,<sup>19,20</sup> the use of absorbents presents other challenges. In most ammonia absorbents, the equilibrium absorption of ammonia in the solid salt absorbent (as represented by absorption isotherms) is nonlinear with varying temperature. This means that the amount of ammonia absorbed by the solid cannot be described by a simple model such as Henry’s law, where the concentration of the target species in the solid varies linearly as the pressure of ammonia.<sup>6,15,16</sup> Rather, the ammonia reacts with the solid with specific stoichiometry similar to the equilibrium behavior for the formation of a hydrated salt.<sup>21</sup> For example, the  $Mg(NH_3)_nCl_2$  salt forms four equilibrium compounds at varying ammonia pressures and temperatures, where  $n$  can be 0, 1, 2, or 6.<sup>11,14,22</sup> The discrete stoichiometric values represent different saturation levels as ammonia is incorporated into the crystal lattice of the salt and are reflected by discrete steps in absorption isotherms.<sup>6</sup> While transitions in levels of metal-salt ammonia saturation have been observed,<sup>21</sup> the curvature in experimental absorption isotherms is a result of kinetic limitations in achieving equilibrium absorption capacities.<sup>16</sup> Ammonia uptake is highly exothermic, and the removal of heat is slow due to the poor thermal conductivity of  $MgCl_2$ . Alternatively, the desorption of ammonia is controlled by ammine decomposition and diffusion of ammonia from the solid to the gas phase.<sup>15,23</sup> The kinetic limitations associated with mass and heat transfer during ammonia absorption and desorption underscore the need for optimized operating conditions to improve the absorbent-enhanced Haber–Bosch

process, especially at a small scale. Here, we take “absorption” to mean uptake and “desorption” to mean release or regeneration.

The optimal design of small-scale Haber–Bosch processes remains to be determined, including the selection of the best method of separating ammonia (condensation, adsorption, or absorption) and associated operating conditions for ammonia capture. Even though there have been some studies on ammonia absorption and desorption using metal halides, these past efforts consist of process conditions that make absorbent-enhanced ammonia synthesis less practical compared to the traditional condensation process.<sup>6,17,23,24</sup> These studies utilized absorption and desorption conditions including uptake times past breakthrough (greater than 50% of breakthrough),<sup>6,17,23,24</sup> high regeneration temperature (400 °C),<sup>6,24</sup> excess sweep gas,<sup>6,17,23,24</sup> and prolonged times (at least an hour)<sup>17,24</sup> for absorbent regeneration. Operating absorbers under these conditions of uptake and release alongside an ammonia synthesis process could prove costly and difficult to implement at small production scales.

The focus of this work is to determine the process conditions that make absorbent-enhanced Haber–Bosch more practical at small scale (<100 tonnes per day). Specifically, we address four key questions: Can the absorbent be effectively regenerated with a lower temperature than 400 °C? Can the absorbent bed be regenerated with minimal or no sweep gas to eliminate a secondary separation step? Can the duration of desorption of ammonia be optimized at a given regeneration temperature? Because previous efforts have used long uptake times, we aim to verify if the salt crystals have higher ammonia loading when uptake is prolonged beyond breakthrough.

To answer these questions, we first evaluated how working capacity was impacted when limiting ammonia uptake for a duration just slightly short of breakthrough (90% of breakthrough) for a range of uptake temperatures. Next, we investigated the performance of the absorbent with variations in regeneration temperature and time. Lastly, we examined the impact of regeneration temperature on the sweep rate and product purity. All of these studies were performed while keeping the absorbent bed size and ammonia partial pressure during uptake constant as in previous studies.<sup>6,23</sup> The findings from this study will drive process design based on minimal utility and less rigorous regeneration conditions required to maintain the comparative cost advantage of the absorbent enhanced process.

## ■ EXPERIMENTAL METHODS

**Materials.** Anhydrous ammonia (99.9% purity), nitrogen (99.9995%), and argon (99.999%) were used as received. In order to make the absorbent, anhydrous magnesium chloride ( $MgCl_2$ , 98%, Sigma-Aldrich), and silica gel ( $SiO_2$ , 60 Å pore size, 70–230 mesh, Sigma-Aldrich) were utilized. Ethanol (99.99%) and methanol (99.98%) were dried with molecular sieves before being used.

**Sample Preparation.** The procedure for making the absorbent material is briefly provided here, however, a more detailed description can be obtained in the previous literature.<sup>17,24</sup> A round-bottom flask was purged with  $N_2$  before adding 30 mL of ethanol and 30 mL of methanol, along with 6 g of anhydrous  $MgCl_2$  (98%, Sigma-Aldrich). This solution was then refluxed for 1 h under a  $N_2$  purge. Also, 9 g of silica gel ( $SiO_2$ , 60 Å pore size, 70–230 mesh, Sigma-Aldrich) was pretreated to remove residual water. This pretreatment involved heating the sample to 450 °C (ramping at 10 °C/min), maintaining this temperature for 10 min, before cooling the sample. After cooling, the sample was immediately added to the  $MgCl_2$  solution. The salt and silica mixture was further refluxed for another 1 h, after which the solvent was removed using vacuum evaporation, while the solid absorbent was dried in a vacuum oven overnight at a temperature of 150 °C.

**Experimental Apparatus.** The experimental apparatus used to evaluate ammonia absorption and desorption was built with stainless steel 316 tubing and fittings from Swagelok. The absorber column had an inner diameter of 1.3 cm and a length of 4.8 cm. Heating tape was wrapped around this metal tube to provide heat as needed. An Omega controller (CN7800) was used to control the temperature during the uptake and regeneration cycles. The control thermocouple was placed in the absorber bed, and a second thermocouple was attached to the outer wall of the metal tube to measure the column wall temperature. Mass flow controllers (model SLA58050S, Brooks Instruments) regulated the flow of nitrogen, argon, and ammonia gases through the absorption column. The pressure in the system was controlled by an Equilibar dome back pressure regulator (model LF05VN12B) that was connected to an Equilibar electronic pressure transducer (model QPV1MANEEZ). System pressure was measured with a pressure transducer (model A-10, WKA) positioned upstream of the absorption column. LabVIEW (National Instruments) software monitored and controlled the process variables in an automated fashion. All instruments and controllers were connected through a NI CRIO-9075 (National Instruments) interface.<sup>6</sup> The composition of the gas mixture exiting the absorber bed was analyzed with a mass spectrometer (SRS RGA 100) which was located further downstream of the absorption column. Further details of the experimental setup can be found in our previous study.<sup>6</sup>

**Experimental Procedure.** About 1.0 g of the absorbent was loaded into the absorber tube. Two stainless-steel plugs were placed at either end of the tube, sandwiching the absorbent to prevent its escape from the column. The absorbent consists of 40 wt %  $MgCl_2$  and 60 wt %  $SiO_2$ .

During the pretreatment phase, the absorbent bed was heated to 400 °C at atmospheric pressure under an  $N_2$  purge (45 standard cubic centimeters per minute, sccm) for 1 h. This was immediately followed by cooling the absorbent to the target absorption temperature (30–200 °C in this study). An

example of the data obtained from the automated cyclic sorption apparatus is shown in Figure 2. After pretreatment, the beginning of the ammonia absorption half-cycle is at point A.

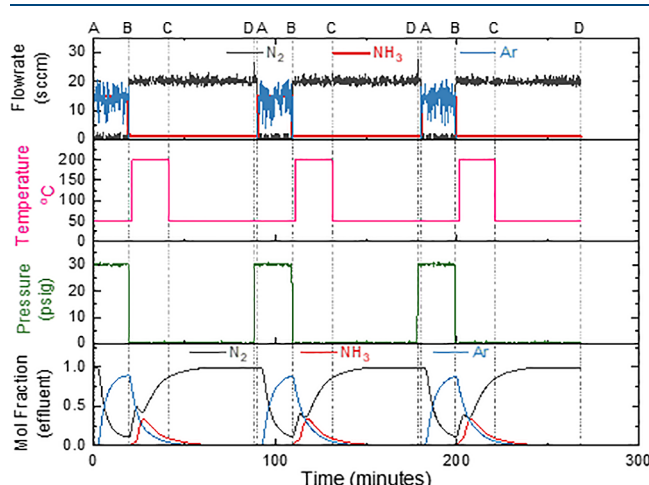


**Figure 2.** Process variables during absorption and desorption cycles (flow rates, set bed temperature, set column gauge pressure, and mole fraction of effluent gas) showing example data from the automated sorption apparatus. A, B, C, and D represent the start of the uptake half-cycle, the start of the desorption half-cycle, the end of the desorption half cycle, and the end of the bed cooling period, respectively. Demonstrates cyclic steady state by the 2nd cycle.

During the absorption phase, the temperature was held constant at the specified absorption temperature; the column pressure was increased to the set pressure (14.5–44.5 psia in this study); the breakthrough experiment began by simultaneously increasing the flow rate of  $NH_3$  and Ar to 15 sccm each while decreasing the  $N_2$  flow to 0 sccm. This low flow rate of  $NH_3$  and Ar is different from the 30 sccm used in our previous paper.<sup>6</sup> The reduced flow rate was selected to ensure a broad time window for  $NH_3$  uptake. Ar flow was used to measure the retention time of a noninteracting or inert gas through the system under all experimental conditions. The partial pressure of  $NH_3$  during absorption was about 23 psi absolute (1.5 bar), which is estimated to be the partial pressure of  $NH_3$  exiting an ammonia synthesis reactor for equilibrium conversion achieved at 290 psi absolute and at 400 °C.<sup>25</sup> The system was maintained at these conditions for a period of time just before breakthrough (an initial experiment was run under the same conditions to determine breakthrough before performing the rerun for a specified time just before the predetermined breakthrough, about 90% of the breakthrough). By preventing breakthrough in this way,  $NH_3$  did not elute the column until during the desorption stage.

During the desorption phase, the flow rates for Ar and  $NH_3$  were turned off while that of  $N_2$  was increased (between 0 and 60 sccm in this study). The desorption half cycle begins at point B as shown in Figure 2. The pressure in the column was also released to atmospheric pressure while the system was purged with  $N_2$ . After equilibrating for 2 min, the bed temperature was increased to the preset desorption temperature (75–200 °C in this study) for the specified desorption time (5–60 min). Readings from the thermocouple inserted inside the absorber column were used to determine the time required for the absorbent bed to reach the specified

temperature. At the end of the specified desorption time, the desorption half-cycle ends and the absorber begins to cool down as indicated by point C in Figure 2.

During the cooling phase, the absorber eventually reaches the absorption temperature ( $50^{\circ}\text{C}$ ) in preparation for the next uptake half-cycle. At the end of the cooling phase, there is a two min wait period before the start of another  $\text{NH}_3$  absorption phase. Point D in Figure 2 indicates the end of the cooling phase.

Three replicate cycles were performed for specific uptake and regeneration conditions before moving on to a new set of variables. Although the process variables change when switching from absorption to desorption, cyclic steady state is achieved by the second cycle as shown in Figure 2 (the area under the curve for  $\text{NH}_3$  mole fraction is identical for cycles 2 and 3). The working capacities published in this report reflect those of the third replicate cycle.

**Calculation of Working Capacity.** In this study, we report measurements of working capacities under different processing conditions. The working capacity is defined as the difference between the capacity of the absorbent after absorption and the capacity after regeneration under operating conditions. The working capacity of the absorbent was calculated by first measuring breakthrough times (time taken for the gas to elute the absorber column) for each absorption cycle. Breakthrough times are defined as the period between the onset of the absorption half cycle and the time points when the partial pressures of  $\text{Ar}$  and  $\text{NH}_3$  reach 0.75% and 1%, respectively. To correct for the system's retention time, the breakthrough for  $\text{Ar}$  was subtracted from that of  $\text{NH}_3$ . Next, we evaluated the amount of  $\text{NH}_3$  absorbed before breakthrough by multiplying the corrected  $\text{NH}_3$  breakthrough with the flow rate of  $\text{NH}_3$  absorbed during absorption. This value was then divided by the appropriate absorbent mass. Unless otherwise stated,  $\text{NH}_3$  absorption was limited to uptake times that were near breakthrough for any given set of operating conditions. This experimental process ensured that the absorbent bed was not fully saturated with ammonia, thus reducing the possibility of ammonia returning to the reactor in an actual ammonia synthesis process.

**Physical Description of the Absorbent.** As shown in Figure 3, the silica support (shards) was observed to be generally larger than the salt particles (gray and grainy) even after subsequent absorption and desorption cycles on the material. We observe the support covered by a salt layer as well as some loose salt particles. It is unclear if the bulk of the sorbent capacity is due to the salt micro crystals which are well

spaced within the pores of the support or the salt layer covering the support or the free salt particles lying outside of the support material. However, since the support materials are generally larger in size than the salt crystals, the salt could still be confined to the interstitial spaces between adjacent silica particles; this promotes the separation of the salt crystals in addition to the space separation attained within the pores of the support, which improves vapor-phase mass transfer.

## RESULTS

**Equilibrium versus Cyclic Steady State Process.** Here, we are interested in process conditions that allow for the largest amount of ammonia per time to be absorbed during uptake and subsequently released with regeneration, as it might be in a small absorbent-enhanced Haber-Bosch plant. It is desirable that such conditions are not only compatible with a low-pressure Haber-Bosch synthesis process but also that they help improve the economic viability and productivity of the absorber-enhanced process compared to the condenser-based one at small scale.

Due to kinetic limitations for ammonia uptake and release using  $\text{MgCl}_2$  supported on  $\text{SiO}_2$ , it is difficult for the ammonia absorbent to achieve equilibrium with the flowing gas and vapors. For example, at  $50^{\circ}\text{C}$  and ammonia pressure above 1.5 bar, the equilibrium capacity is 6 mol  $\text{NH}_3$  absorbed per mole of  $\text{MgCl}_2$ . At  $200^{\circ}\text{C}$  and ammonia pressure below 1 bar, the equilibrium capacity is 2 mol  $\text{NH}_3$  per mole of  $\text{MgCl}_2$ . Thus, the difference in equilibrium capacity is 4 mol  $\text{NH}_3$  per mole of  $\text{MgCl}_2$ . In our experiments described here, the working capacity was more typically  $\sim 2.0$  mol  $\text{NH}_3$  per mole of  $\text{MgCl}_2$ . Of course, any absorptive separation requires a design trade-off between working capacity and process time. The disparity in the capacity measurement results from the long time required to reach equilibrium ammonia absorption in the salt. For these reasons, we designed our experiments to reflect nonequilibrium conditions by operating our absorbent bed in a cyclic steady state.

**Effect of Uptake Temperature on Working Capacity.** To understand the relationship between uptake temperature and the working capacity of the absorbent material, several experiments were conducted where the uptake temperature varied from 30 to  $200^{\circ}\text{C}$ . For each uptake temperature studied, the regeneration temperature, time, and sweep rate were fixed at  $200^{\circ}\text{C}$ , 20 min, and 60 sccm, respectively. Based on equilibrium data in Figure 4, a regeneration temperature of  $200^{\circ}\text{C}$  was chosen, because it was sufficiently high to ensure the “6–2” stoichiometry transition ( $\text{Mg}(\text{NH}_3)_6\text{Cl}_2$  to  $\text{Mg}(\text{NH}_3)_2\text{Cl}_2$ ), for which the equilibrium transition temperature is  $150^{\circ}\text{C}$  at 1.5 bar ammonia pressure. Moreover, prior studies by Kale and co-workers showed that above  $250^{\circ}\text{C}$  regeneration, there was no further increase in the working capacity of  $\text{MgCl}_2$  when uptake was fixed at  $50^{\circ}\text{C}$  and 1.5 bar ammonia pressure.<sup>6</sup> For the “After BT” results, the absorbent was exposed to ammonia for uptake times that were significantly longer (>50%) than the breakthrough time for each absorption temperature. For the “Before BT” results, the absorbent was exposed to ammonia for uptake times that were 90% of the breakthrough time for each absorption temperature.

The measured working capacities are plotted in Figure 5. We also show the working capacities for previous studies conducted by Kale et al. and Hrtus et al., which use longer absorption (uptake of ammonia was past breakthrough, >50%)

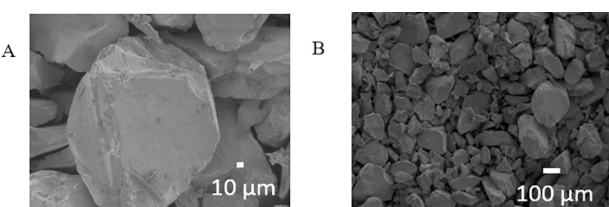


**Figure 3.** Absorbent material (magnesium chloride on silica support) used for ammonia capture in the absorbent-enhanced ammonia synthesis process after multiple cycles of ammonia uptake and release. (A) Magnification 330 $\times$  (B) magnification 80 $\times$ . An SEM micrograph was collected after  $\text{NH}_3$  uptake at  $50^{\circ}\text{C}$  and regeneration for 20 min at  $200^{\circ}\text{C}$ . Column pressure was 30 and 0 psig during  $\text{NH}_3$  uptake and regeneration, respectively.

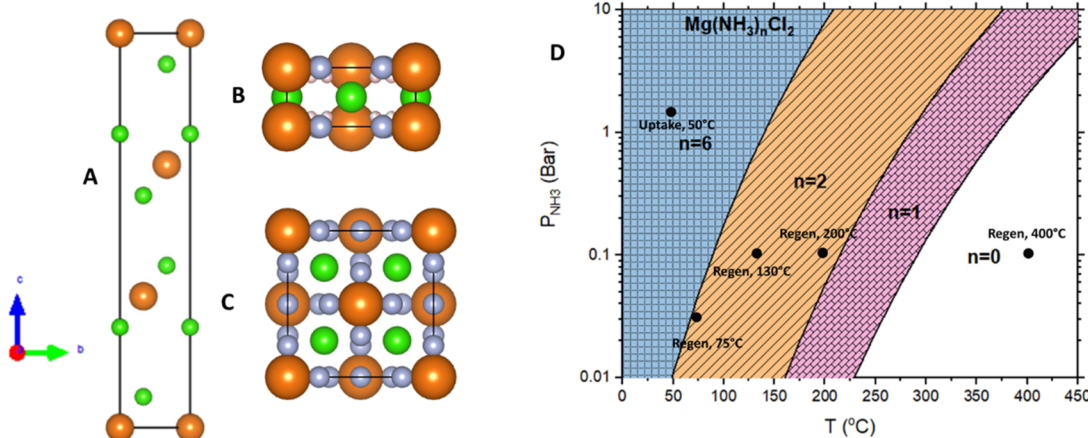


**Figure 4.** Crystal structure for (A)  $\text{MgCl}_2$ , (B)  $\text{Mg}(\text{NH}_3)_2\text{Cl}_2$ , and (C)  $\text{Mg}(\text{NH}_3)_6\text{Cl}_2$  where Cl (green), Mg (brown), N (gray), H (pink), and  $\text{NH}_3$  (gray) in (C), (D) theoretical equilibrium phase diagram for ammoniated  $\text{MgCl}_2$  showing different co-ordination compounds.

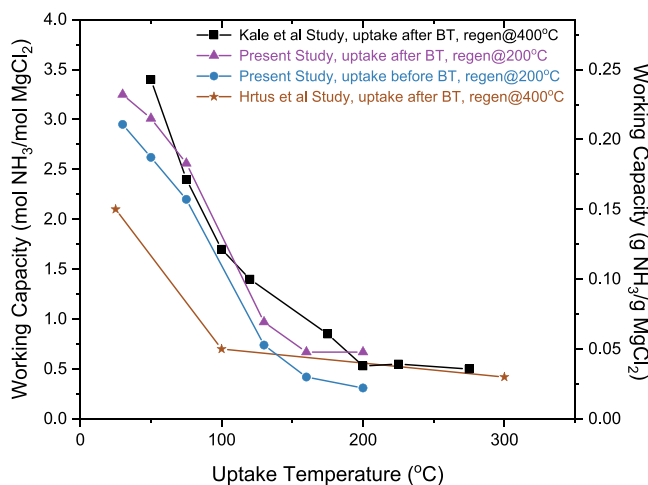


**Figure 5.** Working capacity for: Kale study<sup>6</sup> with long uptake (60 min), higher regeneration temperature (400 °C), and long regeneration time (60 min); present study with long uptake (30 min), lower regeneration temperature (200 °C), and shorter regeneration time (20 min); and present study with short uptake (less than BT time), lower regeneration temperature (200 °C), and short regeneration time (20 min). Data was collected with a sweep rate of 60 sccm (for the duration of regeneration 20 min), and column pressure of 30 and 0 psig during  $\text{NH}_3$  uptake and regeneration, respectively. Hrtus study<sup>26</sup> used long uptake past BT (50 min), less salt at 25 °C, long regeneration of 45 min, and sweep rate of 50 sccm for 3 min. Note: Only specific data from Hrtus et al. that matched our experimental conditions were selected for comparison in this work.

and hotter desorption (regeneration of the bed was performed at a high temperature of 400 °C for an hour).<sup>6</sup> All four curves showed a similar trend as uptake temperature increased; higher working capacity when ammonia was absorbed at lower temperatures. This trend was expected due to the exothermic nature of ammonia absorption.<sup>6,22</sup>

**Effect of Reducing Regeneration Temperature: 200 °C versus 400 °C.** While Figure 5 shows that absorbent capacity increases as the ammonia absorption temperature decreases, it was previously not certain whether this behavior is independent of the regeneration temperature varying from 400 or 200 °C. In addition, Figure 5 shows that the working capacities measured for experiments with 200 °C regeneration are comparable with those at 400 °C. For example, Kale and

co-workers measured a working capacity of about 240 mg  $\text{NH}_3$ /g  $\text{MgCl}_2$  for a 50 °C uptake and 400 °C regeneration while we report a working capacity of about 215 mg  $\text{NH}_3$ /g  $\text{MgCl}_2$  for similar conditions except for a lower regeneration temperature of 200 °C. These new results show that the working capacity can be maintained at a lower regeneration temperature of 200 °C (compared to regeneration at 400 °C) for a whole range of uptake temperatures.

#### Effect of Limiting Uptake Time to Breakthrough

**Time.** Figure 5 shows experimental trials where the uptake times were significantly longer than the breakthrough times for the selected absorption conditions. One disadvantage of operating ammonia uptake past breakthrough is the potential for residual ammonia to be recycled back to the reactor, which would decrease equilibrium yield.<sup>18</sup> With regard to a potential ammonia leak for long uptake times, we then examined whether prolonged ammonia absorption actually increased the absorptive capacity of our absorbent. To evaluate this, the breakthrough times for each individual set of absorption parameters were first determined, and then subsequent ammonia uptake cycles were conducted with uptake times that were 90% of the predetermined breakthrough time. Figure 5 shows that by prolonging ammonia absorption past breakthrough there is no significant increase in the ammonia loading.

Results from other studies show comparable findings and further support our conclusions on minimal additional ammonia loading into the salt when using prolonged uptake times past breakthrough. For example, Hrtus et al. show a trend similar to our results when using analogous operating conditions as shown in Figure 5. They reported the working capacity for  $\text{MgCl}_2$  supported on  $\text{SiO}_2$  as 2.5 mol  $\text{NH}_3$ /mol  $\text{MgCl}_2$  for uptake and regeneration at 25 and 400 °C, respectively, when uptake was well past breakthrough.<sup>26</sup> The working capacity measured by Hrtus and co-workers was lower than our result primarily because the absorbent used was 33 wt %  $\text{MgCl}_2$  rather than 40 wt %, which was utilized in the Kale and Onuoha studies (their shorter sweep time should not affect their capacity much as described below with Figure 10). Also, the temperatures reported are nominal set point temperatures; slight changes in how the absorber column was heated during regeneration could shift the breakthrough curve (this means that ammonia elutes the column at a slightly longer or shorter time). Even though Hrtus and co-workers

absorbed ammonia for a longer time and regenerated the absorbent at a higher temperature, their reported loading of  $\text{NH}_3$  into the salt is still, however, comparable to our measured capacity when the difference in salt fraction is taken into consideration.

**Effect of Further Reducing Regeneration Temperature.** The cost versus benefit of regenerating our absorbent material at a much lower temperature of 200 °C poses a question about the lowest temperature regeneration limit at which the performance of the absorbent material significantly decreases, resulting in a lower overall working capacity of the absorbent bed. To find this lowest regeneration threshold temperature, we examined lower regeneration temperatures of 130 and 75 °C while keeping all other experimental parameters constant.

As shown in Figure 6, the data suggest that with the desorption temperature well below the expected equilibrium

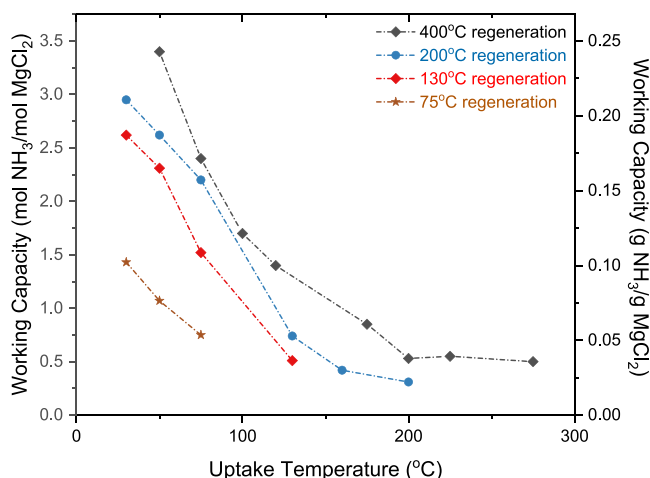


**Figure 6.** Working capacity for previous study with long uptake (60 min), high regeneration temperature (400 °C), and long regeneration time (60 min) to present study with short uptake (less than Breakthrough), short regeneration time (20 min), and lower regeneration temperature (200, 130 and 75 °C). Data were collected with a sweep rate of 60 sccm and column pressure of 30 and 0 psig during  $\text{NH}_3$  uptake and regeneration, respectively.

transition temperature, the accessible working capacity now decreases. The capacity for 200 °C regeneration was almost the same as the 400 °C regeneration because the reduction in the desorption driving force (due to a decrease in regeneration temperature) was not significant enough to affect working capacity. However, further dropping the regeneration temperature below 200 °C does reduce the driving force enough to lower the working capacity.

**Effect of Shortening Desorption Time.** The regeneration temperature fixes the equilibrium pressure of the ammonia in the absorbent bed. Although the partial pressure of ammonia relative to this equilibrium pressure determines whether ammonia is absorbed or released, it does not say how long uptake or release would last. Since working capacity close to the equilibrium capacity could only be achieved at extremely long absorption and regeneration times, it is necessary to investigate the influence of desorption time on the capacity of our absorbent when we operate under cyclic steady state. Regenerating our absorbent for much longer than necessary could result in an extended process time and higher operating costs. The influence of regeneration time on the working

capacity and production capacity of the absorbent was studied and the results are shown in Figures 7 and S2 respectively.

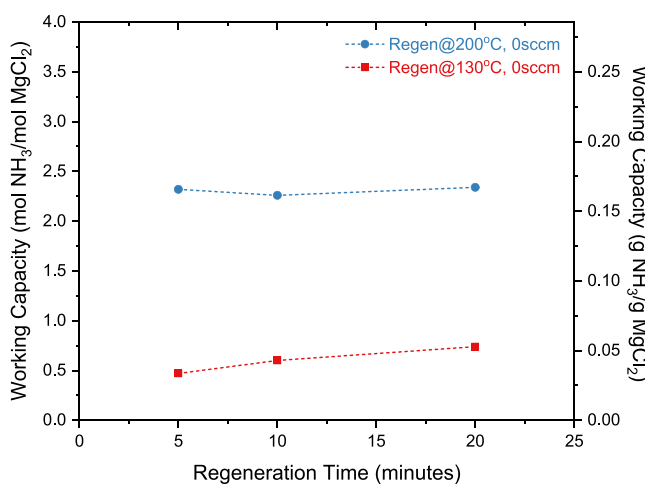


**Figure 7.** Working capacity for uptake just before breakthrough at different regeneration times and temperatures in the presence and absence of sweep gas. Data were collected at an uptake temperature of 50 °C, and column pressure of 30 and 0 psig during  $\text{NH}_3$  uptake and regeneration, respectively.

From Figure 7, regeneration at 200 °C shows no time dependence as the bulk of ammonia is released within a short time (<5 min) regardless of whether the regeneration cycle lasts for 5 or 20 min. This observation is different when we lower the desorption temperature to 130 °C. At a lower regeneration temperature, a longer cycle time is needed for ammonia to desorb from the salt crystals before an appreciable working capacity is reached, which is indicative of a slower desorption rate at a lower regeneration temperature. This is not surprising since at a lower desorption temperature, the distance from equilibrium is smaller than what it would be at a higher temperature assuming all other process variables remain constant. A smaller thermodynamic driving force at a lower regeneration temperature results in a slower desorption rate.

**Effect of the Regeneration Sweep Rate.** Although temperature plays an important role in the absorption and desorption of ammonia in  $\text{MgCl}_2$  by fixing the equilibrium pressure, another important factor is the introduction of sweep gas during desorption, which helps to increase the local desorption driving force. All the results up to this point have used a sweep gas rate of 60 sccm. We investigated the impact of sweep gas when desorption occurs at a reduced column pressure ( $\approx 1$  atm) for different regeneration temperatures.

As shown in Figure 8, we see that sweep gas has minimal impact on working capacity at a high regeneration temperature (200 °C) as the desorption driving force is large. Lowering the regeneration temperature to 130 °C decreases the working capacity by about three-fold, but the working capacity rises significantly when some sweep gas is used to purge the absorber bed. Reducing the regeneration temperature even further to 75 °C results in very minimal desorption such that even with a large sweep, the desorption rate is still slow resulting in a low working capacity.

**Purity and Working Capacity.** Apart from working capacities and ammonia production yields, the performance of our absorbent bed under different process conditions was evaluated based on the purity of the final ammonia product

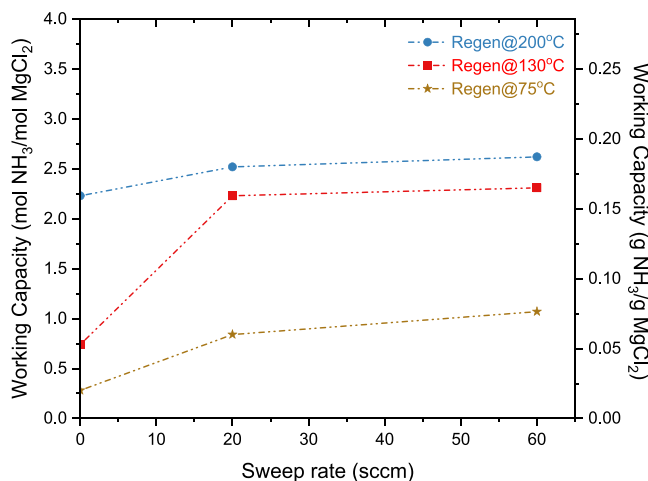


**Figure 8.** Effect of sweep gas rate on working capacity of absorbent material at different desorption temperatures. Data were collected at an uptake temperature of 50 °C, regeneration time of 20 min and column pressure of 30 and 0 psig during NH<sub>3</sub> uptake and regeneration, respectively.

stream. We studied the impact of the regeneration sweep rate and time on ammonia purity.

In Figure 9A, we see that the purity of our ammonia product decreased from 72 to 39 mol % for a 200 °C regeneration under a continuous supply of sweep gas during regeneration, whereas for a 75 °C regeneration purity decreased from 47 to 18 mol % when regeneration time was increased from 5 to 20 min. This result highlights the need to limit the duration of sweep gas if used at all because more ammonia is not necessarily being pushed out of the absorbent material. Figure 9B also shows the impact of the sweep rate on ammonia purity, where the results shown are for the same experimental trials shown in Figure 7. We see that the purity of ammonia decreased dramatically from 100 to 18 mol % for a 200 °C desorption and from 100 to 7 mol % for a 75 °C desorption when a sweep rate of 60 sccm was used. This result further underscores the complementary role sweep gas plays in the release of ammonia from decomposing amminated MgCl<sub>2</sub> crystals. Figure 10 above shows a comparison between a study conducted by Hrtus and co-workers and our own

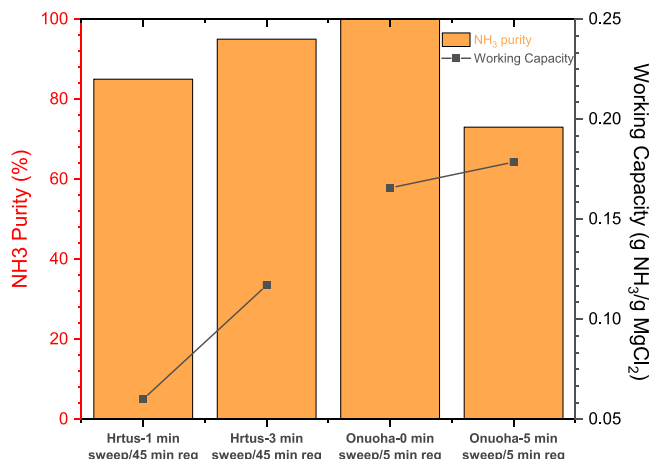


**Figure 10.** Working capacities of our study (Onuoha) where uptake at 50 °C, just before BT, regen at 200 °C, 20 sccm sweep 40 wt % MgCl<sub>2</sub>–SiO<sub>2</sub> and Hrtus study where uptake at 25 °C past BT, regeneration at 200 °C, 50 sccm sweep for 3 min and 20 sccm sweep for 1 min, 33.3% wt % MgCl<sub>2</sub>–SiO<sub>2</sub>.

experiments. The working capacities reported by Hrtus and co-workers are lower than our own values for reasons previously discussed (differences in absorbent composition and regeneration heat rate). When the amount of salt was accounted for between the two studies, the working capacities were comparable. From both results, we can see that for regeneration at 200 °C, the working capacity was close to 190 mg NH<sub>3</sub>/g MgCl<sub>2</sub> of absorbent with a purity level of over 72 mol %. Thus, when the regeneration temperature is sufficiently high, we can get not only a high ammonia capacity yield but also a purer product.

## DISCUSSION

The uptake temperature of the sorbent significantly affected the working capacity. All of the data sets in Figure 5 show a higher working capacity when ammonia is absorbed at lower temperatures. Although this trend is expected due to the exothermic nature of ammonia absorption,<sup>6,22</sup> it was previously not certain whether this behavior depended on the regeneration temperature, especially when regenerating the

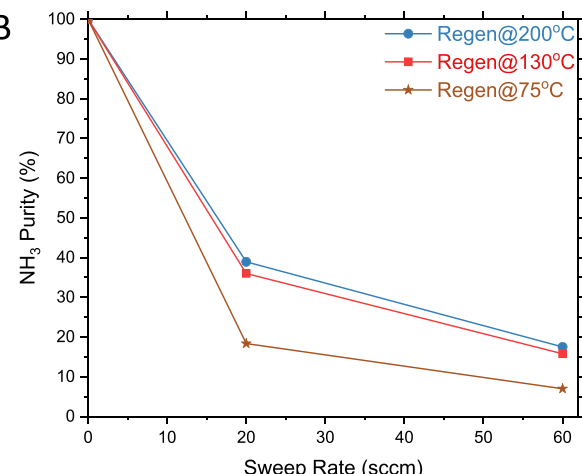
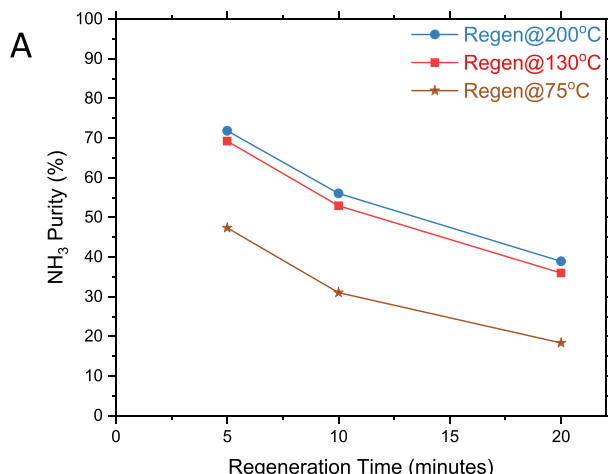


**Figure 9.** Absorption column effluent purity level for uptake at 50 °C lasting just before BT (A) for a sweep rate of 20 sccm at different regeneration times (B) for different sweep rates at a regeneration of 20 min.

absorbent at a significantly lower temperature (compared to 400 °C used in previous studies; for consistent comparison, data were collected in the same uptake time of about 1 h).<sup>6,24</sup> It is worth noting though that for the 200 °C regeneration curve, as the uptake temperature falls below 50 °C, the observed increase in bed capacity becomes less sensitive to temperature. This lower sensitivity at low temperatures might be due to the onset of a kinetic limitation associated with a slower recrystallization rate of hexa-ammine salt. The lowest sorbent bed ammonia uptake temperature one would try to use while avoiding process chilling is 50 °C.

We also examined the effect of decreasing the sorption bed regeneration temperature. In Figure 5, we showed that regenerating the absorber bed at 200 °C resulted in a working capacity comparable to that obtained using 400 °C. However, a regeneration temperature of 75 °C resulted in much smaller working capacities as shown in Figure 6. The data of Figure 4 explain why desorption at 75 °C is no longer favored to sufficiently drive out ammonia resulting in lower working capacity; the equilibrium pressure of ammonia for a “6 to 2” ammoniated salt transition increases sharply with temperature, so there is a larger desorption driving force for desorption at 400 or 200 °C compared to 75 °C. The driving force for ammonia transfer into and out of the sorbent is proportional to the vertical distance from each state in Figure 4 (fixed ammonia pressure and temperature). With the sweep gas rate used here, we expected the bulk partial pressure of ammonia to be much less than 0.1 bar. Here, the driving force for ammonia released at 75 °C was extremely low. Desorption is no doubt enabled only by the use of sweep gas removing the ammonia, reducing its partial pressure in the absorbent bed. Desorption might also be assisted by the higher-than-bulk-equilibrium partial pressure afforded by small-dispersed salt particles and by small temperature excursions by the controller over the nominal temperature.

Figure 4, however, challenges us to explain why 400 °C desorption does not perform even better than the measured sorbent bed performance. It suggests that using a regeneration temperature of 400 °C could, at equilibrium, completely regenerate the absorbent ( $\text{Mg}(\text{NH}_3)_6\text{Cl}_2$  to  $\text{MgCl}_2$ ) and yield a capacity of about 420 mg  $\text{NH}_3/\text{g MgCl}_2$ , but we and others report only about 240 mg  $\text{NH}_3/\text{g MgCl}_2$  even with a large sweep rate and long desorption time. Given that the working capacity we observe for a 200 °C regeneration is similar to that for a 400 °C regeneration, we infer that achieving full desorption to ammonia-free  $\text{MgCl}_2$  is likely kinetically (mass diffusion) limited. This idea is supported by other experiments which report no additional ammonia desorbed at temperatures above 325 °C.<sup>6</sup> The difficulty in completely regenerating the absorbent ( $\text{Mg}(\text{NH}_3)_6\text{Cl}_2$  to  $\text{MgCl}_2$ ) might be a result of the lower driving force for ammonia desorption as the absorbent approaches the fully ammonia-free form.<sup>16</sup>

Being able to regenerate the  $\text{MgCl}_2$  absorbent as well at a lower temperature of 200 °C as opposed to 400 °C has significant benefits for the absorbent-enhanced renewable ammonia process. Palys et al. have shown that high-temperature regeneration (>400 °C) accounts for about 80% of the operational cost of the absorbent enhanced process at small scale and slows the use of the absorbent bed with excessive bed temperature swing.<sup>9</sup> Although not included in this report, a techno-economic analysis (TEA) would be needed to balance the benefits of lower utility cost savings and time needed to heat the column to the set point against the

loss of working capacity below 200 °C. For our current study, we will continue with 200 °C regeneration, since it is a sufficiently high temperature to desorb ammonia and yield high working capacities.

Before proceeding to other sorbent bed operating parameters, we note that we found that it does not matter much to the measured working capacity if the uptake time exceeds the breakthrough time. In practice, the absorber would be operated with an uptake time just short of breakthrough to avoid permitting ammonia return to the synthesis reactor. But in many studies, uptake times routinely exceeded breakthrough; our current concern is whether the extra uptake time used in our previous work might have allowed so much time for extra ammonia absorption (e.g., reaching less accessible salt), thus increasing the working capacity beyond one that can be achieved practically in a real process. It is reassuring, though, as shown in Figure 5, that stopping short of breakthrough produces no significant decrease in the working capacity for the 200 °C regeneration. Data presented in Figures 7–9 use only uptake times limited to the measured breakthrough time.

There are several factors that might explain why prolonging ammonia absorption past breakthrough does not increase the ammonia loading into the absorbent material. The uptake reaction is exothermic, so there will always be small temperature increases at the absorption front as it moves down the bed; therefore, one possibility is that the uptake is spontaneous (the exothermicity of ammonia uptake raises the temperature and ensures there is enough energy to overcome the activation barrier for recrystallization of ammoniated salt) at the reaction front, helping ensure a sharp breakthrough. Further ammonia uptake after breakthrough does not benefit from this thermal acceleration and might only increase the net absorbed amount slowly. On the other hand, full uptake of the sorbent with ammonia requires the sorbent to swell to a substantially larger volume (the hexamine form requiring more volume),<sup>27</sup> so it is also possible that some of the salt remains inaccessible; this would also limit any capacity increase with further uptake time.

Another process variable explored was the sorbent bed regeneration time, which at a given breakthrough time will set the cycle time and influence the net throughput rate of the cycling absorbent bed.<sup>6</sup> An optimal absorption–desorption process might involve fast cycling of the absorbent bed to take advantage of a faster initial desorption rate experienced early in the regeneration half-cycle.<sup>17,28</sup> As shown in Figure 7, decreasing the regeneration time from 20 to 5 min at a regeneration temperature of 200 °C resulted in the same working capacity. The bulk of ammonia was released within the first few minutes of the start of the desorption cycle, with only a small amount desorbing after 5 min. However, when the regeneration temperature was lowered to 130 °C, ammonia release was slower; therefore, longer regeneration times were required to obtain reasonable working capacities. A high regeneration temperature has the advantage of a higher thermodynamic driving force for ammonia release and a higher rate of diffusion, so faster cycling was possible. Using a shorter regeneration time can increase the production capacity (ammonia processed per unit absorbent and per unit production time) and so can allow for the use of smaller columns (which can also be heated and cooled faster). Smaller beds can be used to cycle faster multiple times resulting in higher ammonia product yield; they can also avoid the capital

cost and heat transfer difficulties presented by larger beds.<sup>6</sup> On the other hand, excessively high regeneration temperatures can add unnecessarily long wait times and utility costs (to heat and cool between cycles). Figure S2 (in the Supporting Information) shows that the production output using 50 °C uptake and 200 °C regeneration can be increased up to 4-fold when decreasing the regeneration from 20 to 5 min. These results are significant as fast cycling can be a useful design strategy (balancing, of course, the added complexity of faster cycling including temperature and pressure swings).

The fourth process variable is the rate of sweep gas used during regeneration of the absorbent, which can increase the working capacity. The convective flow provided by the sweep gas decreases the partial pressure of ammonia in the bulk gas, providing additional driving force for ammonia desorption.<sup>16</sup> However, this same dilution of the bulk gas requires further purification of the product stream. In seeking an optimum process, the absorbent would be regenerated using minimal sweep gas to prevent the need for a secondary separation unit for this absorbent-enhanced process. As shown in Figure 8, the benefit of sweep gas depends on the regeneration temperature. Using 200 °C as regeneration temperature, a large working capacity can be obtained with no sweep gas at all; using 130 °C would require a large sweep rate to yield high capacity, and for 75 °C even larger sweep rates cannot produce the expected working capacity. At 200 °C, there is sufficient driving force to drive ammonia out of the absorbent, so the rate of desorption benefits little from the sweep gas (as shown in Figure 8). Others have also shown (using similar absorbent and uptake temperatures) that there is little benefit to using much sweep gas when using sufficiently high regeneration temperature (greater than 200 °C)<sup>26</sup> and have attributed the benefit of high desorption temperature to the formation of nanopores within the salt particles which creates a transport pathway to the bulk gas.<sup>11</sup>

Since there is an additional cost of using excess sweep and a need for a secondary purification unit,<sup>8</sup> it is favorable to regenerate the absorbent material at the lowest temperature that practically eliminates the need for sweep. For this reason, 200 °C would likely be selected in a practical design, and a complete process design and economic analysis should give full consideration for this design trade-off, and its economic impact will inform a suitable process path.

We also emphasize that optimizing the operation should take into account the purity of the regeneration stream. Figure 10 shows that the absorbent bed can be regenerated without sweep gas (if the temperature is high enough), which would yield the purest product. If the absorbent bed can be regenerated with little or no sweep gas (by using a sufficiently high regeneration temperature) this would avoid any need for purification from the sweep gas. It is helpful to use a regeneration temperature that is adequately high to avoid the need for excessive sweep, but not necessarily any higher.

## CONCLUSIONS

The research described here aims to enable distributed ammonia to be synthesized more efficiently by using the standard Haber–Bosch catalyst with an improved ammonia separation method using a cyclically operating high-temperature ammonia absorber. If operated efficiently, this can allow ammonia to be made at a lower pressure<sup>10,18</sup> and lower capital cost; it may also be more suitable for smaller-scale production than the conventional large-scale process.

In this work, we experimentally evaluated the impact on absorber performance of the following variables: ammonia uptake temperature, uptake time, regeneration temperature, regeneration sweep gas rate, and regeneration time. Here, we show that absorbent regeneration using very high temperatures (>400 °C) is unnecessary and may be inefficient in terms of utility cost and wait time to reach target temperatures.<sup>9</sup> The cost and energy efficiency of the absorbent-enhanced process is further complicated when a significant flow rate of inert sweep gas is used. Here, we show that while a large rate of sweep gas such as nitrogen can be useful to drive the desorption of ammonia from the absorbent material, in practice too much sweep is unnecessary and would necessitate a secondary purification step to obtain a pure ammonia product. Finally, we show that unnecessarily long desorption times become less effective at separating ammonia and will limit the number of separation cycles that can be operated, resulting in less ammonia produced per unit of production time.<sup>6</sup>

Our understanding of the impact of these process variables will guide process optimization, improving the economic viability of this process especially at smaller production scales.<sup>9</sup> Further work is needed to explore the effect of the scale of the process such as the impact of using larger absorbent beds. In addition, a process design and economic analysis will be able to utilize the operational parameter evaluation to optimize the economic and production potential of an ammonia processing facility using an ammonia absorber.

## ASSOCIATED CONTENT

### Supporting Information

The Supporting Information is available free of charge at <https://pubs.acs.org/doi/10.1021/acs.iecr.3c04351>.

Graph showing the working capacity for uptake just before breakthrough and desorption at different times with sweep gas as well as bed temperature throughout the ammonia uptake and release cycles; production rate (working capacity per unit regeneration time) for uptake just before breakthrough at different regeneration temperatures in the presence and absence of sweep gas; normalized concentration curve for ammonia absorption into  $MgCl_2$  supported on  $SiO_2$ ; optical micrographs showing the absorbent material (magnesium chloride on silica support) used for ammonia capture in the absorbent-enhanced ammonia synthesis process; and table showing our results for ammonia uptake and release using  $MgCl_2$  based absorbent compared to other published studies (PDF)

## AUTHOR INFORMATION

### Corresponding Author

Alon V. McCormick – Department of Chemical Engineering & Materials Science, University of Minnesota, Minneapolis, Minnesota 55455, United States;  [orcid.org/0000-0002-8885-1330](https://orcid.org/0000-0002-8885-1330); Email: [mccormic@umn.edu](mailto:mccormic@umn.edu)

### Authors

Chinomso E. Onuoha – Department of Chemical Engineering & Materials Science, University of Minnesota, Minneapolis, Minnesota 55455, United States;  [orcid.org/0000-0003-4156-4649](https://orcid.org/0000-0003-4156-4649)

Matthew J. Kale – Department of Chemical Engineering & Materials Science, University of Minnesota, Minneapolis,

Minnesota 55455, United States;  [orcid.org/0000-0002-3039-3111](https://orcid.org/0000-0002-3039-3111)

Mahdi Malmali – Department of Chemical Engineering, Texas Tech University, Lubbock, Texas 79409, United States;  [orcid.org/0000-0001-5190-1261](https://orcid.org/0000-0001-5190-1261)

Paul J. Dauenhauer – Department of Chemical Engineering & Materials Science, University of Minnesota, Minneapolis, Minnesota 55455, United States;  [orcid.org/0000-0001-5810-1953](https://orcid.org/0000-0001-5810-1953)

Complete contact information is available at:

<https://pubs.acs.org/10.1021/acs.iecr.3c04351>

## Funding

This work was funded in part by the Advanced Research Projects Agency-Energy (ARPA-E), U.S. Department of Energy, under award no. DE-AR0000804; in part by the U.S. Department of Energy's Office of Energy Efficiency and Renewable Energy (EERE) under the Advanced Manufacturing Office Award Number DE-EE0007888; in part by the Office of the Vice President for Research, University of Minnesota; and in part by University of Minnesota West Central Research and Outreach Center through the State of Minnesota Renewable Development Account. The views and opinions of the authors expressed in this report are not necessarily reflective of the United States Government or other governmental agencies. The authors thank Michael Reese, Zac Pursell, Sameer Parvathikar, Matthew Palys, and Ed Cussler for helpful discussions.

## Notes

The authors declare no competing financial interest.

## ■ REFERENCES

- (1) Erisman, J. W.; Sutton, M. A.; Galloway, J.; Klimont, Z.; Winiwarter, W. How a century of ammonia synthesis changed the world. *Nat. Geosci.* **2008**, *1*, 636–639.
- (2) Klerke, A.; Christensen, C. H.; Norskov, J. K.; Vegge, T. Ammonia for hydrogen storage: challenges and opportunities. *J. Mater. Chem.* **2008**, *18*, 2285–2392.
- (3) Angeles, D. A.; Are, K. R.; Aviso, K. B.; Tan, R. R.; Razon, L. F. Optimization of the automotive ammonia fuel cycle using P-graphs. *ACS Sustain. Chem. Eng.* **2017**, *5*, 8277–8283.
- (4) Zhang, T.; Miyaoka, H.; Miyaoka, H.; Ichikawa, T.; Kojima, Y. Review on Ammonia Absorption Materials: Metal Hydrides, Halides, and Borohydrides. *ACS Appl. Energy Mater.* **2018**, *1*, 232–242.
- (5) Gilbert, P.; Alexander, S.; Thornley, P.; Brammer, J. Assessing economically viable carbon reductions for the production of ammonia from biomass gasification. *J. Clean. Prod.* **2014**, *64*, 581–589.
- (6) Kale, M. J.; Ojha, D. K.; Biswas, S.; Militi, J. I.; McCormick, A. V.; Schott, J. H.; Dauenhauer, P. J.; Cussler, E. L. Optimizing Ammonia Separation via Reactive Absorption for Sustainable Ammonia Synthesis. *ACS Appl. Energy Mater.* **2020**, *3*, 2576–2584.
- (7) Lin, B.; Norwin, F. H.; Rosenthal, J. J.; Bhowm, A. S.; Malmali, M. Perspective on Intensification of Haber–Bosch to Enable Ammonia Production under Milder Conditions. *ACS Sustainable Chem. Eng.* **2023**, *11*, 9880 DOI: [10.1021/acsuschemeng.2c06711](https://doi.org/10.1021/acsuschemeng.2c06711).
- (8) Reese, M.; Marquart, C.; Malmali, M.; Wagner, K.; Buchanan, E.; McCormick, A. V.; Cussler, E. L. Performance of a Small-Scale Haber Process. *Ind. Eng. Chem. Res.* **2016**, *55*, 3742–3750.
- (9) Palys, M. J.; McCormick, A.; Cussler, E. L.; Daoutidis, P. Modeling and Optimal Design of Absorbent Enhanced Ammonia Synthesis. *Processes* **2018**, *6*, 91.
- (10) Malmali, M.; Reese, M.; McCormick, A. V.; Cussler, E. L. Converting Wind Energy to Ammonia at Lower Pressure. *ACS Sustain. Chem. Eng.* **2018**, *6*, 827–834.
- (11) Hummelshøj, J. S.; Sørensen, R. Z.; Kustova, M. Y.; Johannessen, T.; Nørskov, J. K.; Christensen, C. H. Generation of Nanopores during Desorption of NH<sub>3</sub> from Mg(NH<sub>3</sub>)<sub>6</sub>Cl<sub>2</sub>. *J. Am. Chem. Soc.* **2006**, *128*, 16–17.
- (12) Elmoe, T. D.; Sørensen, R. Z.; Quaade, U.; Christensen, C. H.; Nørskov, J. K.; Johannessen, T. A high-density ammonia storage/delivery system based on Mg(NH<sub>3</sub>)<sub>6</sub>Cl<sub>2</sub> for SCR–DeNO<sub>x</sub> in vehicles. *Chem. Eng. Sci.* **2006**, *61*, 2618–2625.
- (13) Annable, D. Application of the Temkin kinetic equation to ammonia synthesis in large-scale reactors. *Chem. Eng. Sci.* **1952**, *1*, 145–154.
- (14) Aoki, T.; Miyaoka, H.; Inokawa, H.; Ichikawa, T.; Kojima, Y. Activation on Ammonia Absorbing Reaction for Magnesium Chloride. *J. Phys. Chem. C* **2015**, *119*, 26296–26302.
- (15) Smith, C.; McCormick, A. V.; Cussler, E. L. Optimizing the Conditions for Ammonia Production Using Absorption. *ACS Sustain. Chem. Eng.* **2019**, *7*, 4019–4029.
- (16) Smith, C.; Malmali, M.; Liu, C. Y.; McCormick, A. V.; Cussler, E. L. Rates of Ammonia Absorption and Release in Calcium Chloride. *ACS Sustain. Chem. Eng.* **2018**, *6*, 11827–11835.
- (17) Wagner, K.; Malmali, M.; Smith, C.; McCormick, A.; Cussler, E. L. Column Absorption for Reproducible Cyclic Separation in Small Scale Ammonia Synthesis. *AIChE J.* **2017**, *63*, 3058–3068.
- (18) Malmali, M.; Wei, Y.; McCormick, A.; Cussler, E. L. Ammonia Synthesis at Reduced Pressure via Reactive Separation. *Ind. Eng. Chem. Res.* **2016**, *55*, 8922–8932.
- (19) Lin, B.; Wiesner, T.; Malmali, M. Performance of a Small-Scale Haber Process: A Techno-Economic Analysis. *ACS Sustain. Chem. Eng.* **2020**, *8*, 15517–15531.
- (20) Nowrin, F. H.; Malmali, M. Optimizing Reaction-Absorption Process for Lower Pressure Ammonia Production. *ACS Sustain. Chem. Eng.* **2022**, *10*, 12319–12328.
- (21) Liu, C. Y.; Aika, K. Ammonia Absorption on Alkaline Earth Halides as Ammonia Separation. *Bull. Chem. Soc. Jpn.* **2004**, *77*, 123–131.
- (22) Sørensen, R. Z.; Hummelshøj, J. S.; Klerke, A.; Reves, J. B.; Vegge, T.; Nørskov, J. K.; Christensen, C. H. Indirect, Reversible High-Density Hydrogen Storage in Compact Metal Ammine Salts. *J. Am. Chem. Soc.* **2008**, *130*, 8660–8668.
- (23) Ojha, D. K.; Kale, M. J.; Dauenhauer, P. J.; McCormick, A.; Cussler, E. L. Desorption in Ammonia Manufacture from Stranded Wind Energy. *ACS Sustain. Chem. Eng.* **2020**, *8* (2020), 15475–15483.
- (24) Malmali, M.; Le, G.; Hendrickson, J.; Prince, J.; McCormick, A. V. Better Absorbents for Ammonia Separation. *ACS Sustainable Chem. Eng.* **2018**, *6*, 6536–6546.
- (25) Nielsen, A.; Kjaer, J.; Hansen, B. Rate equation and mechanism of ammonia synthesis at industrial conditions. *J. Catal.* **1964**, *3*, 68–79.
- (26) Hrtus, D. J.; Nowrin, F. H.; Lomas, A.; Fotsa, Y.; Malmali, M. Achieving + 95% Ammonia Purity by Optimizing the Absorption and Desorption Conditions of Supported Metal Halides. *ACS Sustain. Chem. Eng.* **2022**, *10*, 204–212.
- (27) Bevers, E.; Oonk, H.; Haije, W.; Van Ekeren, P. Investigation of thermodynamic properties of magnesium chloride amines by HPDSC and TG: For application in a high-lift high-temperature chemical heat pump. *J. Therm. Anal. Calorim.* **2007**, *90*, 923–929.
- (28) Veselovskaya, J. V.; Tokarev, M. M.; Aristov, Y. I. Novel ammonia sorbents ‘porous matrix modified by active salt’ for adsorptive heat transformation. I. Barium chloride in various matrices. *Appl. Therm. Eng.* **2010**, *30*, 584–589.